Proceedings of Global Power and Propulsion Society
ISSN-Nr: 2504-4400
GPPS Hong Kong 2023
October 17-19, 2023
www.gpps.global

GPPS-TC-2023-0273

Axial Compressor Design System with Direct Generation of 3D Geometry

Milan Banjac, Djordje Petkovic, Teodora Madzar, Milan V. Petrovic
Faculty of Mech. Engineering
University of Belgrade
mbbanjac@mas.bg.ac.rs
Belgrade 11120, R. Serbia

ABSTRACT

This paper presents a software system for the design of axial compressors assembled from several modular tools. The central feature is the possibility to generate a complete 2D and 3D design in a single run, using a basic set of general and stage-related parameters. This results in a geometry definition that can be analyzed with commercial CFD tools. The number of stages and the blade geometry are determined through the computing procedure, which preserves the input mean line parameters. Complementary programs can be used to evaluate the overall off-design performance and to examine and modify individual cascade sections before time-consuming CFD computations are engaged. Each tool is accompanied by a graphical interface for more accessible data analysis. The design examples and comparisons are demonstrated.

INTRODUCTION

Although mean line and two-dimensional aerodynamic computer programs have been present for an extended period, the accuracy and universality of such codes are often limited due to the application of simple loss models. Such loss models are calibrated to be suited for a specific range of configurations used by a company, and the initial design is refined through other methods, such as CFD. The main goal of the present research was to generate universal design and analysis codes that produce reliable results for any axial configuration. The design system generates 1D mean line design, which is refined with 2D throughflow design procedure. The output is used to create complete 3D geometry for CFD analysis or mechanical evaluations. All the steps are done in a single pass, while any phase can be revisited to make the improving corrections. However, the usage of a reliable and flexible loss model minimizes the needed number of revision steps. The additional tools analyze the blade-to-blade flow and off-design compressor performance.

DEVELOPMENT

Analysis Method and the Loss Model

The initial research related to 2D compressor analysis (Petrovic et al., 2009) included the adaptation of stream function-based turbine code (Petrovic, 1995) and the development of appropriate loss model (Banjac et al., 2014, 2015). The cascade loss and deviation are computed according to Lieblein (1965); Pfitzinger (1998); Aungier (2003), and the secondary effects using the correlations from Denton (2014); Lakshminarayana (1970); Roberts et al. (1986). The end wall boundary layer and the operational stability are evaluated as in Jansen (1967); Waltke (1995) and Aungier (2003). Recently, a state-of-the-art shock loss and choking limit model (Banjac et al., 2022) was added. Thus far, the code has been validated on more than 20 test cases, including several multistage geometries presented in (Banjac et al., 2015), transonic fans such as Moore and Reid (1980); Strazisar et al. (1989); Hirsch and Denton (1981), and non-public cases (LTTUB, 2009*a*,*b*, 2022), incorporating the configurations with up to 17 stages. Each major revision of the loss model is re-validated using all of the foregoing test cases.

Design Method

Simultaneously, the loss model was utilized for a design tool presented in a two-part paper Banjac and Petrovic (2018*a*,*b*). The iterative mean line procedure determines the required number of stages and their geometry according to the general and stage-related performance parameters. The thermodynamic process is computed along the mean line, including all relevant planes in each stage, and the needed cascade operating parameters and geometry are computed. At the same time, an analytical vortex solution determines hub and tip velocity triangles. This evaluates the required cascade

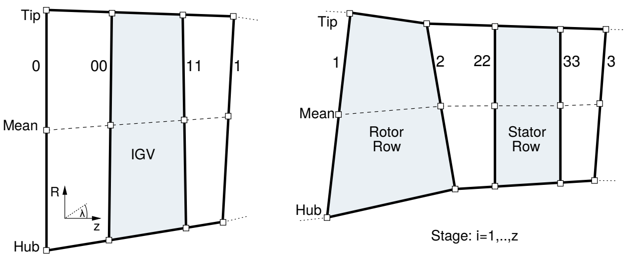

Figure 1 Mean line method representation

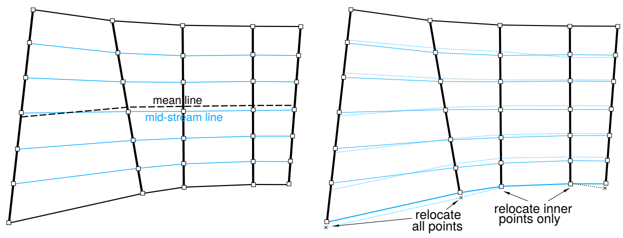

Figure 2 Two dimensional representation

geometry at the hub and tip. Therefore, a realistic flow path shape is obtained using polygons, as shown in Figure 1. In such a way, 1D mean line design produces a rough 3-section-based 2D design. The row heights are determined by the resulting densities and axial velocities. Sizing in rotor row-related planes 1 and 2 results from stage flow and loading coefficients. The stator block 2-3, which consists of the row and the adjacent ducts, provides the required guidance for the following stage.

Unlike the matrix-based stream function analysis tool, the 2D design code applies the streamline curvature method, more suitable for required geometry manipulations inside the design procedure iterations (Figure 1). The mean line solution is now refined using a complete radial equilibrium equation being integrated, combined with spline-defined end wall boundaries (Banjac and Petrovic, 2018*b*). Once again, planes 1 and 2 are sized to preserve mean line flow and loading parameters. The integration process matches the required velocities at the mean line position, while the end wall boundaries are relocated to satisfy the mass flow conditions (Figure 2). The geometry of stator row leading and trailing edge stations 22 and 33 is obtained by interpolation to provide smooth guidance to the following stage. Then, the radial equilibrium integration is performed with fixed endpoints, and only the internal streamlines are relocated.

Blade Modeling

The 3D blade geometry is generated using a parametric design tool for turbines and compressors. Airfoil sections are created by connecting four Non-Uniform Rational B-Spline (NURBS) curves (Piegl and Tiller, 1996). For the suction and pressure side, 4th-degree NURBS curves are used (Figure 3). The leading edge is modeled as an ellipse, while the trailing edge is a circle. The connecting points are 3rd order continuous, except for the trailing edge, which is connected with 1st degree continuous junctions. There are seven airfoil shapes used for the input of classical geometric data. Some contain fixed geometry, such as NACA 65, while others use a variable position of maximum thickness and camber. The input data are inlet and outlet camber angles, relative thickness, maximum arrow position, leading and trailing edge radii, as well as the chord. The method to parameterize an input geometry is based on a modified approach of Pritchard (1985), where certain parameters are replaced to adopt the approach for the compressor airfoil. Introduced parameters are related to the ellipse-shaped leading edge, inlet and outlet semi-wedge angles, and additional pressure and suction side points, bringing the parameter count to 17. Together with six additional parameters related to the derivatives in the junctions and the added pressure and suction side points. These parameters are generated automatically and can be manually modified, exported, or loaded directly. Finally, the 3D shape is obtained by interpolating all parameters across the span. This is done using a 5th order natural B-spline curve to allow a variable number of final sections, which are by default stacked using a straight axis.

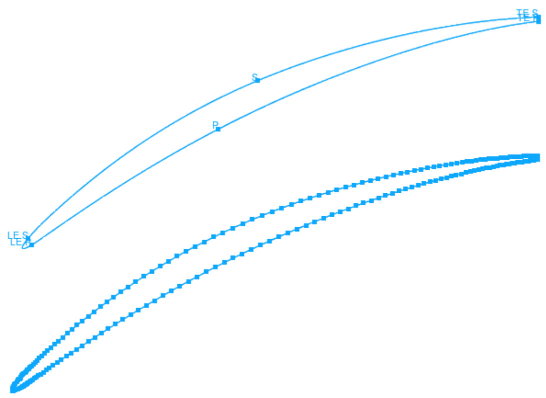

Figure 3 Parametric and discretized airfoil representation

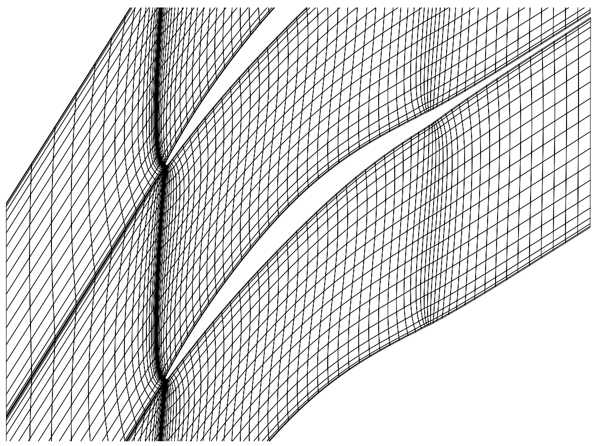

Figure 4 Blade-to-blade numerical grid

Blade-to-Blade Flow Analysis

On a desired row section, the blade-to-blade flow can be analyzed using two dimensional S1 surface flow solver. The main free-stream solver employs the time-marching JST finite volume scheme (Jameson, 2017), applied on a revolving stream sheet with variable thickness and inertial forces acting.

The grid is structured and consists of the inlet, profile, and outlet blocks (Figure 4). Quasi-orthogonal stations are generated using a 3rd degree, while the quasi-tangential lines are created with 2nd degree B-spline curves. The density of stations is increased with the higher curvature of the profile contours (Thompson, 1999), near the block boundaries, as well as in the vicinity of the open trailing edge. The grid is then smoothed using the elliptic smoothing (Karman, 2010).

The boundary layer and wake impact are modeled by the usual transformation of the effective airfoil shape according to the local displacement thickness. The integral compressible boundary layer and wake equations and solved by Newton's method using closure relations from Drela (1986, 1989). The indirect mode is applied, where the displacement thickness is prescribed, and the end velocity is calculated and compared with the free stream velocity. The wake sides are observed together as a single viscous layer, and the endpoints are relocated to equalize the upper and lower pressure. The transition location is predicted with the combination of AGS and e^n criteria (Drela, 1986).

SYSTEM STRUCTURE INCLUDED TOOLS

The structure of the design system is shown in Figure 5, and it contains:

- **acmean**, the main design tool which provides the following functions:
  - 1D mean line design,
  - 1D mean line off-design analysis,
  - 2D design,
- **bgeom**, 3D blade geometry generation,
- **cflow**, blade-to-blade flow analysis at design or off-design conditions,
- **acflow**, 2D off-design analysis,

Each program has the accompanying graphical interface shown (Figure 5), while **bgeom** is a graphical application itself.

The **acmean** always executes the 1D design procedure. If specified, an additional option is then performed in a single program run. In the case of the 1D performance analysis, the program generates the mean line design and directly applies given off-design operating conditions, thus eliminating the need to export geometry to an external program. The same principle is applied in the case of the 2D mode. This procedure takes the mean line solution as the initial case and eventually outputs an additional set of 2D design-related files.

The blade geometry modeler **bgeom** is a graphical program that loads 2D blade section and flow path data and creates spline-based blade shape and flow path. The 3D clouds of points are then exported to be used for CFD analysis or mechanical evaluations. The geometry can be modified by changing the values of spline parameters. The additional output contains the classical mechanical parameters for each blade section, such as moments of inertia, etc. The effectiveness of generated airfoil shapes can be examined using blade-to-blade flow solver **cflow**.

The 2D compressor flow analysis program **acflow** is a well-documented tool used for compressor off-design analysis and generation of compressor maps for transient simulations. In combination with the gas turbine analysis code, the overall engine performance simulation can be performed (Petrovic and Wiedermann, 2013).

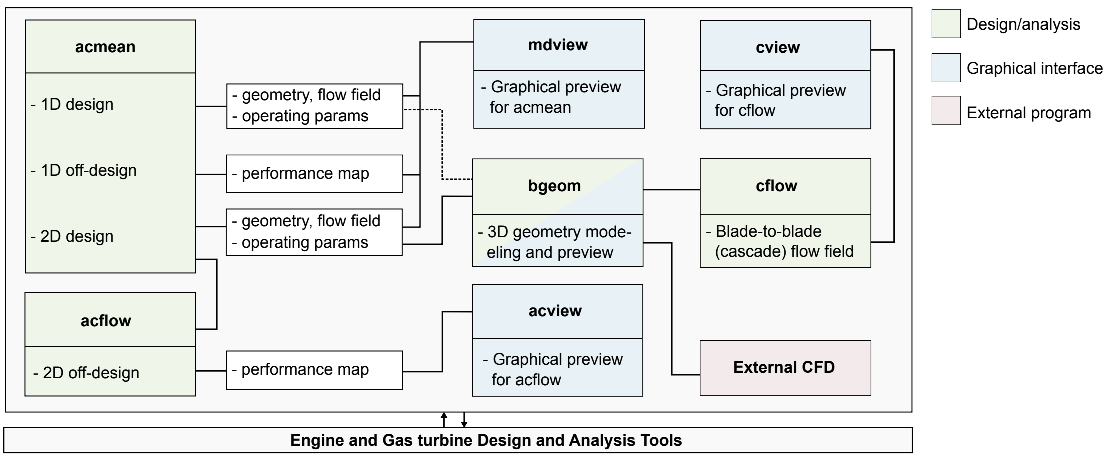

Figure 5 Compressor design system scheme

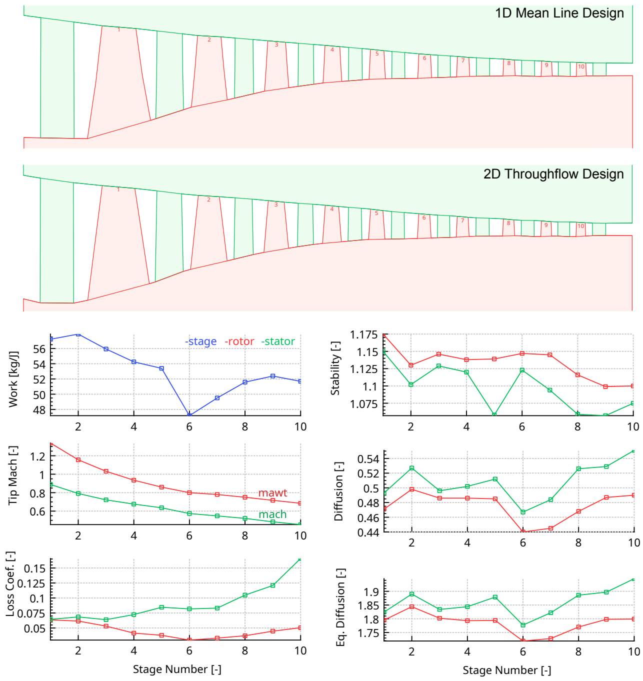

Figure 6 Flow path and basic stage parameters

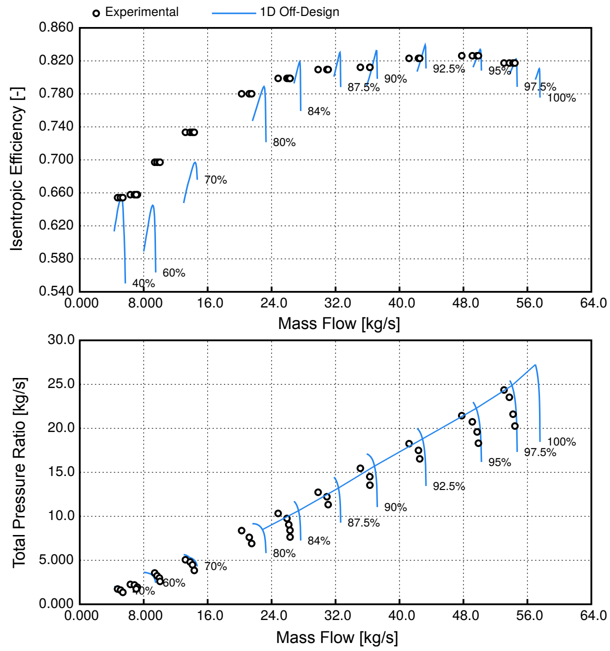

Figure 7 Performance map

GENERAL DESIGN AND ANALYSIS

A compressor design case is generated using an input file that contains the following sets of data:

- **general:** mass flow, pressure ratio, inlet blockage, etc.
- **first rotor inlet plane:** tip Mach number, rotor speed, and diameter ratio, of which two are used
- **flow path shape:** constant hub, constant tip, constant mean diameter or given tip diameter distribution
- **stage parameters:** distribution of flow and loading coefficients, solidity, aspect ratio, clearances, etc.

When the program is run, the needed number of stages is determined automatically in the first few iterations. The stage parameters are given as arrays, and if the number of stages exceeds the array size, the last value is used for excessive stages. All the parameters are preserved during the iterative run except for the stage loading coefficients. These must be corrected so that the configuration with an integer number of stages produces an exact value of the given total pressure ratio, and the members of the stage loading coefficient array are scaled proportionally. If a repeating stage concept is used, the input contains single-member stage arrays of stage properties.

The design method is demonstrated by reconstructing the well-known test case from Holloway et al. (1982). Figure 6 shows the difference between the 1D and 2D design and the distribution of selected mid-span stage parameters. As mentioned before, the 2D design procedure retains the mid-span flow angle and flow coefficient, and the stage loading is again scaled to fit the total pressure ratio into the desired value, which is mainly related to a difference in the prediction of losses between 1D and 2D procedures. The off-design mode can be used to directly produce a compressor performance map (Figure 7). Alternatively, the 2D off-design analysis tool can be used, as demonstrated later.

The parameters of the first rotor inlet plane significantly influence the overall configuration. For example, a variation of the tip Mach number changes the flow path, as shown in Figure 8. Figure 9 shows the resulting distributions of the stage loading coefficient. In the example, the Mach number was varied in the narrow range to produce an identical stage count in all the solutions.

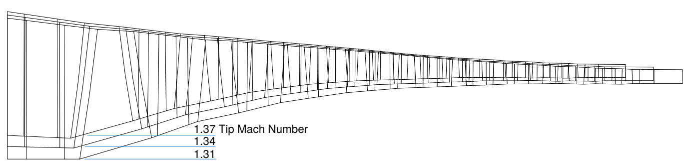

Figure 8 Variation of tip Mach number

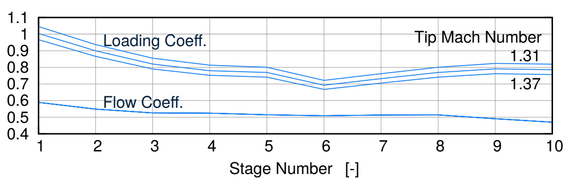

Figure 9 Influence on stage loading coefficients

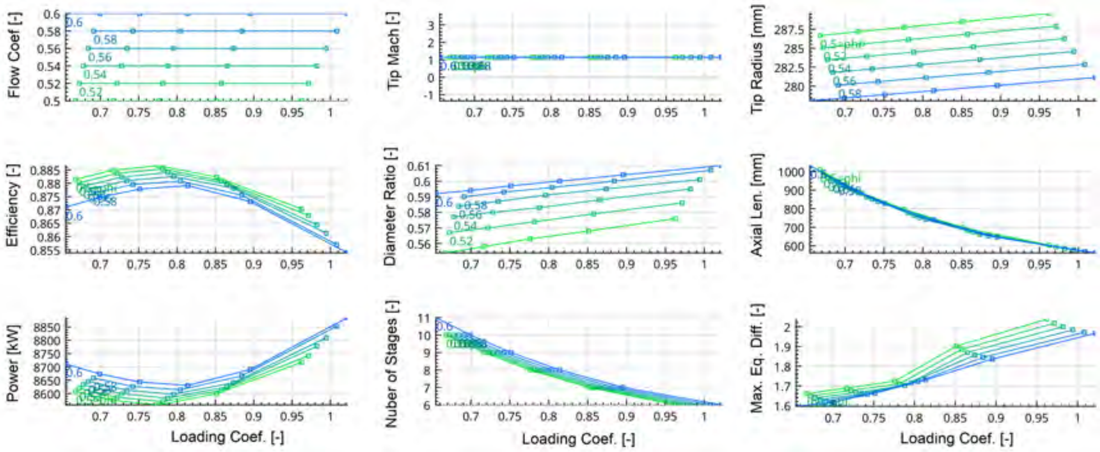

Figure 10 Preview of flow and loading coefficient variation

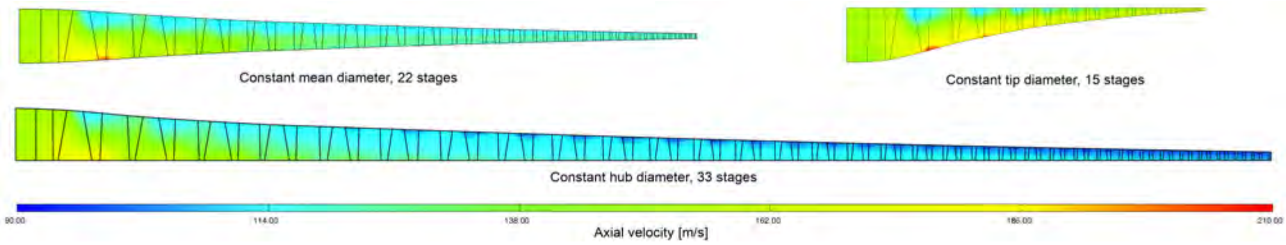

Figure 11 Outputs generated by 2D design for pressure ratio of 40

Some variations can be done using built-in loops, for example, the change of stage and loading coefficients. This produces a set of complete 1D solutions collectively shown in Figure 10. Such a preview is used to determine an optimal choice of basic parameters. When the general parameters are selected, the program can be started with the 2D design option, and the numerical procedure generates an additional set of output files with 2D design data and geometry. For example, Figure 11 demonstrates three different 2D solutions. These were created using identical input data, except for the option regarding the basic flow path shape. Optionally, a 2D solution can be modified without changing the mean concept using an additional input file, which modifies spanwise distributions of parameters such as work and swirl. Also, the automatic radial distribution of geometric parameters, such as the chord and thickness, can be altered.

CASCADE FLOW ANALYSIS AND BLADE REDESIGN

The blade modeler loads 2D section data and generates parameterized spline airfoils for each spanwise position. A particular section can be modified to correct the airfoil shape and obtain a better curvature distribution along the contour and, thus, a better performance (Figure 12). Since a large number of input sections is hard to manipulate, only a few active

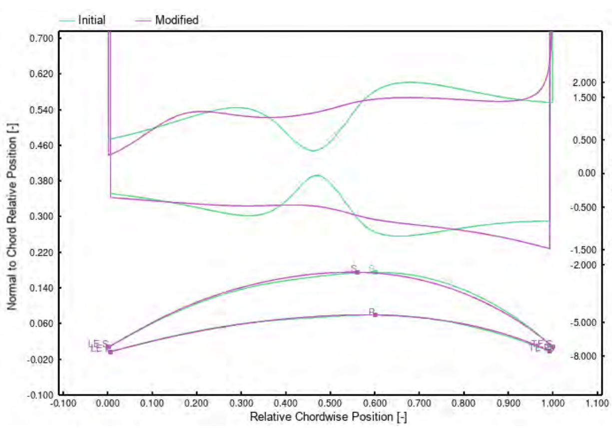

Figure 12 Modification of airfoil geometry

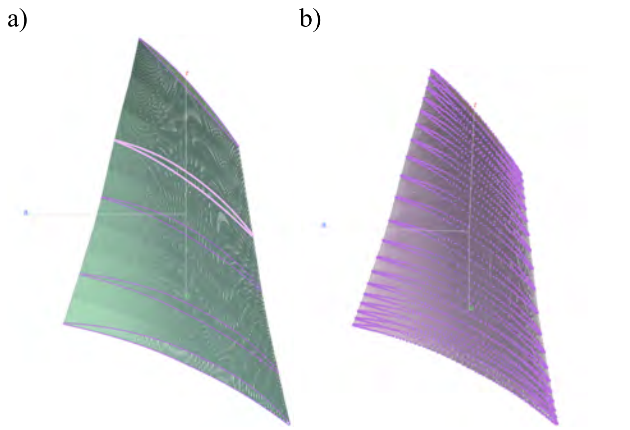

Figure 13 Active profiles and exported cloud of points

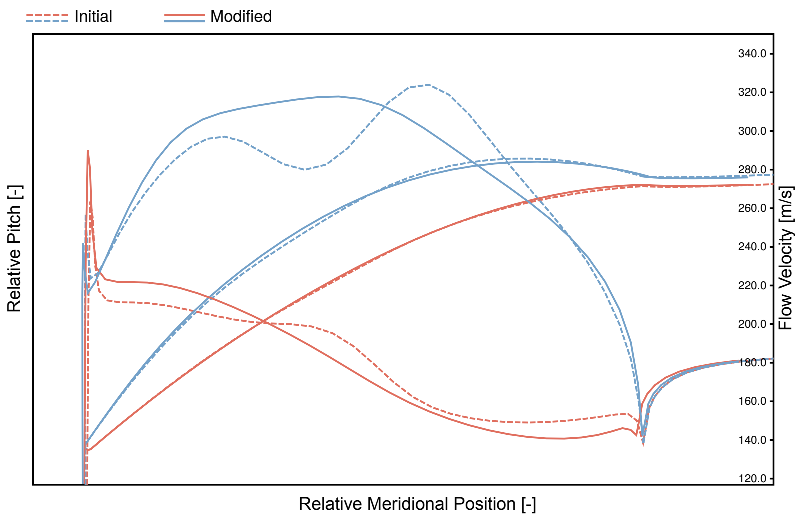

Figure 14 Profile velocity distribution

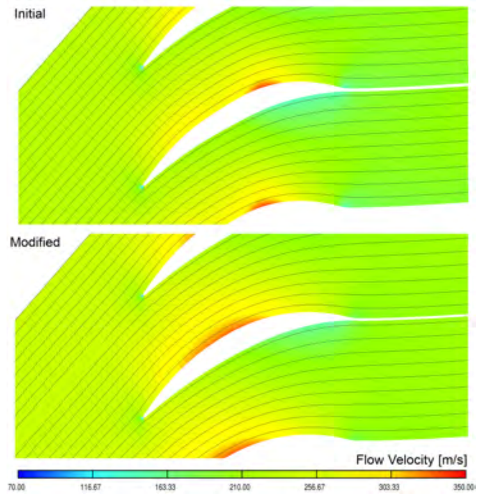

Figure 15 Blade-to-blade flow field

segments are used to modify the geometry (Figure 13-a). Correction of any parameter in an active section is then interpolated between active locations and redistributed to all input positions. In such a way, correction is applied to all airfoils using a limited number of sections to be analyzed and modified. The 3D geometry is then exported using an adjustable number of sections and points per profile in a point cloud (Figure 13-b).

Then, the input file for the blade-to-blade flow solver is exported for a selected blade section. After the solving procedure, the cascade flow field and overall performance parameters are obtained. It can be determined if cascade geometry produces desired outflow angle and efficiency demanded by the general 2D design. Even if the overall cascade performance parameters are satisfying, the airfoil can be reshaped (Figure 14) to produce a better velocity or pressure distribution across the contour, as shown in Figure 15. The modification, data exporting, and re-calculation can be performed rapidly. Analyzed conditions correspond to the nominal operation by default but can be altered.

EXAMPLE CASE

This configuration was produced to demonstrate the accuracy of the method and not to create a high-end design. The nominal total pressure ratio and the mass flow are 9 and 30 kg/s, respectively. The original case presented in Banjac and Petrovic (2018*b*) was slightly changed to produce a higher stall margin since a corner stall prediction method of Yu and Liu (2010) was added to the program in the meantime. This modification relates only to the increase of blade solidity in specific stator rows. Flow path dimensions can be seen in Figure 16. All rows are unshrouded, and the tip clearances are 0.5 mm for the rotor and 0.8 mm for the stator rows. Used profiles are Multiple Circular Arc for the rotor and NACA 65 for stator rows. The flow path shape and the blade geometry can be seen in Figure 17. The 2D solution runs for about 10 seconds on a 2.2 GHz processor.

The meridional flow field produced by the 2D design method is shown in Figure 18. The performance of exported 3D geometry is validated with commercial CFD. The simulation was performed with CFX solver (ANSYS, 2023), applying single blade mixing plane RANS model $k-\omega$ turbulence model and the wall functions. The circumferentially averaged flowfield is given in Figure 19. The high-speed zones introduced by the blade blockage can not be seen in the 2D design results (Figure 18) since the method does not include internal computational stations. However, the influence of the blade blockage is in detail considered inside the loss model by the previously mentioned shock loss and choking limit model

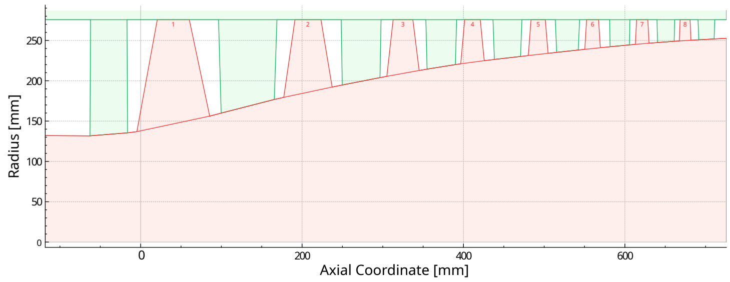

Figure 16 Flow path shape

Figure 17 Blade shapes, first three stages

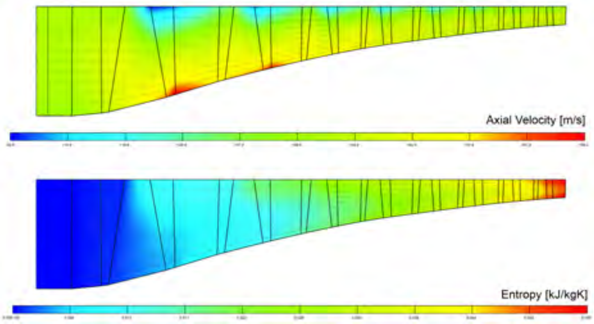

Figure 18 Meridional flow field, 2D design

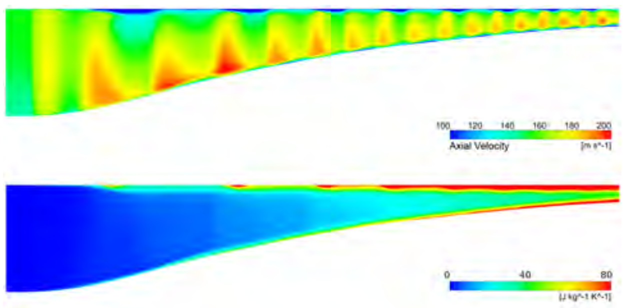

Figure 19 Meridional flow field, CFD

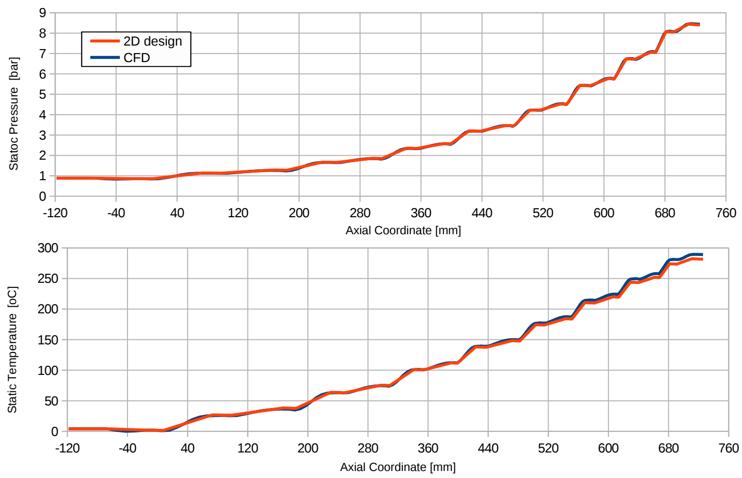

Figure 20 Streamwise distribution of pressure and temperature

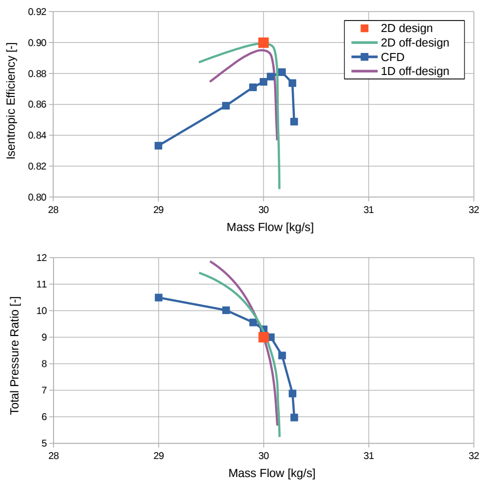

Figure 21 Performance map

(Banjac et al., 2022). Moreover, if choking is detected during the iterative computations, the geometry of the choked airfoil section is automatically modified to allow an increased mass flow. The results are also compared in Figure 20. The performance map in Figure 21 shows prediction by 1D and 2D design and off-design methods, as well as CFD. The agreement for the pressure ratio curve is excellent. A slight disagreement of efficiency of the order of 2% is the consequence of the inability of the mixing plane approach to introduce a realistic amount of spanwise mixing, thus generating highly uneven spanwise distribution of entropy in the rear stages.

CONCLUSIONS

This paper presents a software system for the design of axial fans and multistage compressors. It includes several tools for 1D and 2D aerodynamic design and analysis, 3D blade geometry modeling and the cascade flow analysis. All codes are equipped with corresponding graphical postprocessors. The mean tool for 1D and 2D design, together with the blade modeler, allows the generation of 3D geometry in a single run using mean line data only. Of course, any phase of the design procedure can be revisited and additionally considered to improve the final solution. The tools are validated using a large number of experimental cases and CFD results, and some examples are demonstrated.

References

ANSYS (2023), www.ansys.com.

Aungier, R. H. (2003), *Axial-Flow Compressors, A Strategy for Aerodynamic Design and Analysis*, ASME Press, New York.

Banjac, M. and Petrovic, M. V. (2018*a*), 'Development of Method and Computer Program for Multistage Axial Compressor Design: Part I — Mean Line Design and Example Cases', *ASME Paper* **GT2018-75410**.

Banjac, M. and Petrovic, M. V. (2018*b*), 'Development of Method and Computer Program for Multistage Axial Compressor Design: Part II — Two-Dimensional Design and Validation Using CFD', *ASME Paper* **GT2018-75412**.

Banjac, M., Petrovic, M. V. and Wiedermann, A. (2014), 'A New Loss and Deviation Model for Axial Compressor Inlet Guide Vanes', *ASME Journal of Turbomachinery* **136(7)**.

Banjac, M., Petrovic, M. V. and Wiedermann, A. (2015), 'Secondary Flows, Endwall Effects and Stall Detection in Axial Compressor Design', *ASME Journal of Turbomachinery* **137(5)**.

Banjac, M., Savanovic, T., Petkovic, D. and Petrovic, M. V. (2022), 'A Comprehensive Analytical Shock Loss Model for Axial Compressor Cascades', *Journal of Turbomachinery* **144**(9).

Denton, J. D. (2014), 'Loss Mechanisms in Turbomachines', *ASME Journal of Turbomachinery* **115**, 621–656.

Drela, M. (1986), *Two-dimensional transonic aerodynamic design and analysis using the Euler equations*, Gas Turbine Laboratory, Massachusetts Institute of Technology, Cambridge, Massachusetts.

Drela, M. (1989), 'Integral Boundary Layer Formulation for Blunt Trailing Edges', *7th Applied Aerodynamics Conference* .

Hirsch, C. and Denton, J. D. (1981), 'Through Flow Calculations in Axial Turbomachines', *AGARD Report* **AR-175**, 229–255.

Holloway, P. R., Knight, G. L., Koch, C. C. and Shaffer, S. J. (1982), 'Energy Efficient Engine High Pressure Compressor Detail Design Report', *NASA Report* **CR-165558**.

Jameson, A. (2017), 'Origins and Further Development of the Jameson–Schmidt–Turkel Scheme', *AIAA Journal* **55**(5), 1487–1510.

Jansen, W. (1967), 'The Application of End-Wall Boundary Layer Effects in the Performance Analysis of Axial Compressors', *ASME Paper* **67-WA/GT-11**.

Karman, S. L. (2010), Virtual Control Volumes for Two-Dimensional Unstructured Elliptic Smoothing, *in* 'Proceedings of the 19th International Meshing Roundtable', Springer Berlin Heidelberg, Berlin.

Lakshminarayana, B. (1970), 'Methods of Predicting the Tip Clearance Effects in Axial Flow Turbomachines', *ASME Journal of Basic Engineering* **92**, 467–482.

Lieblein, S. (1965), 'Experimental Flow in Two-Dimensional Cascades in: Aerodynamic Design of Axial-Flow Compressors, by Johnsen, I. A. and Bullock, R. O.', **NASA Report**, 183–225.

LTTUB (2009*a*), Aerodynamic calculation and Flow Analysis of 11-Stage MaBoKo Compressor, Technical report, Lab. of Thermal Turbomachinery, University of Belgrade – Faculty of Mechanical Engineering.

LTTUB (2009*b*), Aerodynamic Calculation and Flow Analysis of 17-Stage Sulzer Compressor, Technical report, Lab. of Thermal Turbomachinery, University of Belgrade – Faculty of Mechanical Engineering.

LTTUB (2022), Software System for Aerodynamic Design and Analysis of Axial Compressors, Technical report, Lab. of Thermal Turbomachinery, University of Belgrade – Faculty of Mechanical Engineering.

Moore, R. D. and Reid, L. (1980), 'Performance of Single-stage Axial-flow Transonic Compressor with Rotor and Stator Aspect Ratios of 1.19 and 1.26 Respectively, and with Design Pressure Ratio of 2.05', *NASA Report* **NASA-TP-1659**.

Petrovic, M. V. (1995), *Berechnung der Meridian Stroemung in mehrstufigen Axialturbinen bei Nenn- und Teillastbetrieb*, number Reihe 7, Nr. 280, VDI-Verlag, Duesseldorf.

Petrovic, M. V. and Wiedermann, A. (2013), 'Through-Flow Analysis of Air-Cooled Gas Turbines', *ASME Journal of Turbomachinery* **135**(6).

Petrovic, M. V., Wiedermann, A. and Banjac, M. (2009), 'Development and Validation of a New Universal Throughflow Method for Axial Compressors', *ASME Paper* **GT2009-59938**.

Pfitzinger, W. E. (1998), *Kennfeldberechnung fuer Axialverdichter mit systematischer Untersuchung der Verlust und Umlenkeigenschaften von Schaufelgittern*, number Reihe 7 Nr. 337, VDI-Verlag, Duesseldorf.

Piegl, L. A. and Tiller, W. (1996), *The NURBS Book*, Springer Science Business Media.

Pritchard, L. (1985), 'An Eleven Parameter Axial Turbine Airfoil Geometry Model', *ASME Paper* **85-GT-219**.

Roberts, W. B., Serovy, G. K. and Sandercock, D. M. (1986), 'Modeling the 3-D Flow Effects on Deviation Angle for Axial Compressor Middle Stages', *ASME Journal of Engineering for Gas Turbines and Power* **108**, 131–137.

Strazisar, A. J., Wood, J. R., Hathaway, M. D. and Suder, K. L. (1989), 'Laser anemometer measurements in a transonic axial-flow fan rotor', *NASA Report* **NASA TP-2879**.

Thompson, J. F. (1999), *Handbook of Grid Generation*, CRC Press LLC.

Waltke, U. (1995), *Berechnung des Meridianströmungsfeldes in Axialverdichtern mit der Methode der Finiten Elemente*, number Reihe 7, Nr. 261, VDI-Verlag.

Yu, X. and Liu, B. (2010), 'A Prediction Model for Corner Separation/Stall in Axial Compressors', *ASME Paper* **GT2010-22453**.